Conditional Overexpression of Connective Tissue Growth Factor Disrupts Postnatal Lung Development

Shu Wu[1], Astrid Platteau[1], Shaoyi Chen[1], George McNamara[2], Jeffrey Whitsett[3], and Eduardo Bancalari[1]

[1]Department of Pediatrics, Division of Neonatology, and [2]Analytical Imaging Core Facility, University of Miami Miller School of Medicine, Miami, Florida; and [3]Division of Pulmonary Biology, Cincinnati Children's Hospital Medical Center, Cincinnati, Ohio

Connective tissue growth factor (CTGF) is a member of an emerging family of immediate-early gene products that coordinates complex biological processes during development, differentiation, and tissue repair. Overexpression of CTGF is associated with mechanical ventilation with high tidal volume and oxygen exposure in newborn lungs. However, the role of CTGF in postnatal lung development and remodeling is not well understood. In the present study, a double-transgenic mouse model was generated with doxycycline-inducible overexpression of CTGF in respiratory epithelial cells. Overexpression of CTGF from Postnatal Days 1–14 resulted in thicker alveolar septa and decreased secondary septal formation. This is correlated with increased myofibroblast differentiation and disorganized elastic fiber deposition in alveolar septa. Overexpression of CTGF also decreased alveolar capillary network formation. There were increased α–smooth muscle actin expression and collagen deposition, and dramatic thickening in the peribronchial/peribronchiolar and perivascular regions in the double-transgenic lungs. Furthermore, overexpression of CTGF increased integrin-linked kinase expression, activated its downstream signaling target, Akt, as well as increased mRNA expression of fibronectin. These data demonstrate that overexpression of CTGF disrupts alveologenesis and capillary formation, and induces fibrosis during the critical period of alveolar development. These histologic changes are similar to those observed in lungs of infants with bronchopulmonary dysplasia.

Keywords: connective tissue growth factor; transgenic; postnatal lung; development

CLINICAL RELEVANCE

This work demonstrates that overexpression of connective tissue growth factor during the critical alveolar developing period disrupts alveolarization and capillary formation and induces fibrosis in mice. These results provide new insights into the molecular mechanisms of postnatal lung development and the pathogenesis of bronchopulmonary dysplasia.

Despite recent advances in neonatal intensive care and surfactant therapy, bronchopulmonary dysplasia (BPD) remains a major cause of morbidity and mortality in extremely premature infants (1). The lung pathology of BPD is characterized by decreased alveolarization, dysmorphic capillary formation, and variable interstitial fibrosis (2, 3). Increasing evidence suggests that BPD is the consequence of developmental arrest of the immature lung in response to injury and deranged repair processes (4, 5). Therefore, better understanding of the molecular mechanisms of postnatal lung development and remodeling will provide new insights into the pathogenesis of BPD, and open the possibility of novel preventive and therapeutic strategies.

Many studies indicate that transforming growth factor (TGF)–β is a potential causal factor in the pathogenesis of BPD (6, 7). Transgenic overexpression of TGF-β in the lungs of newborn mice results in alveolar hypoplasia and fibrosis resembling BPD-like architecture (8). Connective tissue growth factor (CTGF), a prototypical member of the CCN family of proteins, is closely related to TGF-β (9). The CCN family contains six members of early gene products (CTGF/Fisp12, Cyr61/Cef10, Nov, rCOP-1/WISP-1, Elm-1/WISP-2, and WISP-3), with a high degree of amino acid sequence homology and 38 conserved cysteine residues (10–12). CTGF is a ligand of the integrin complexes (13). Integrin-linked kinase (ILK) is a serine/threonine kinase that couples integrins to downstream signaling pathways, leading to activation of a diverse array of cellular processes, including cell adhesion, proliferation, migration, differentiation, extracellular matrix (ECM) production, and angiogenesis (14–19). CTGF is best known for its role as a downstream mediator and a coactivator of TGF-β fibrogenic effects. Overexpression of CTGF and TGF-β were found in many forms of adult pulmonary fibrosis in clinical studies and animal models (20–22). Increasing evidence suggests a potential role of CTGF in embryonic and neonatal lung development and remodeling. A recent study has shown that CTGF gene expression is increased in mouse lungs from Postnatal Days 14 to 28, correlating with increased abundance of phopho-Smad2, an intracellular TGF-β–signaling transducer (23). Studies from our laboratory have demonstrated that TGF-β induces CTGF expression in the mesenchyme of embryonic lung explants, and CTGF inhibits branching morphogenesis (24). We and other investigators have demonstrated that mechanical ventilation with high tidal volume and hyperoxia exposure upregulates CTGF expression in newborn rat lung, suggesting a role of CTGF in postnatal lung injury and repair (25, 26). CTGF gene mutation in mice results in newborn death with respiratory failure due to rib cage deformity and lung hypoplasia (27, 28). However, the exact role of CTGF in postnatal lung development and remodeling remains to be defined.

Much of the knowledge on lung development has been generated through studies using transgenic mouse models with lung tissue–specific expression of target genes directed by gene promoter of surfactant protein (SP-C) or Clara cell secretory protein (CCSP) (29). To determine the role of CTGF in postnatal lung development, we have generated a doxycycline-inducible double-transgenic mouse model with conditional overexpression of CTGF in respiratory epithelial cells directed by the CCSP gene promoter. Our data demonstrate that overexpression of CTGF in the postnatal lung disrupts alveolarization, decreases capillary formation, and induces fibrosis. Thus, overexpression of CTGF in airway epithelium leads to lung

(*Received in original form February 20, 2009 and in final form May 29, 2009*)

This work was supported by funding from National Institutes of Health grant K08 HD046582, a Bank of America charitable grant, Project Newborn from the University of Miami, and the Micah Batchelor Award from the Batchelor Foundation.

Correspondence and requests for reprints should be addressed to Shu Wu, M.D., Department of Pediatrics, Division of Neonatology, University of Miami Miller School of Medicine, P.O. Box 016960, Miami, FL 33101. E-mail: swu2@med.miami.edu

Am J Respir Cell Mol Biol Vol 42. pp 552–563, 2010
Originally Published in Press as DOI: 10.1165/rcmb.2009-0068OC on June 18, 2009
Internet address: www.atsjournals.org

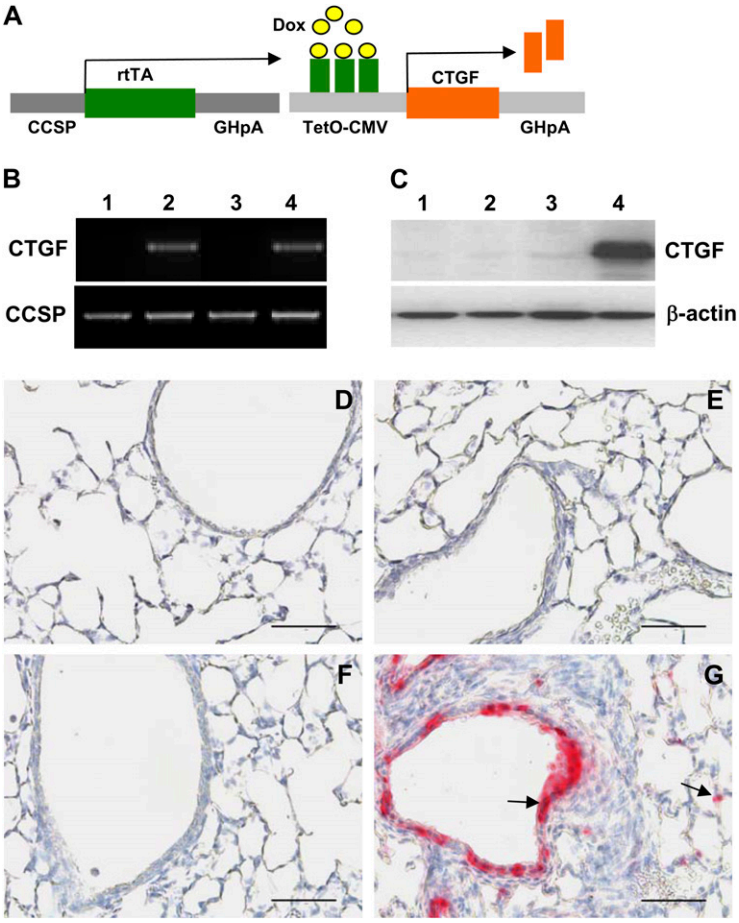

Figure 1. Generation of double-transgenic mouse model with conditional overexpression of connective tissue growth factor (CTGF) in respiratory epithelium. (*A*) Mating homozygous Clara cell secretory protein (CCSP)–reverse tetracycline-responsive transactivator (rtTA) mice to heterozygous tetracycline operator (TetO)–CTGF mice produced double-transgenic pups containing CCSP-rtTA and TetO-CTGF transgenes. Administration of doxycycline (Dox) to the dams from Postnatal Days 1–14 induced overexpression of CTGF in airway epithelium. (*B*) PCR analysis of tail DNA with CCSP-rtTA and TetO-CTGF primers identified CCSP-rtTA single-transgenic (STG) mice (*lanes 1* and *3*) and CCSP-rtTA/TetO-CTGF double-transgenic (DTG) mice (*lanes 2* and *4*) without (*lanes 1* and *2*) and with (*lanes 3* and *4*) Dox administration. (*C*) Western blot analysis demonstrated high level of CTGF protein expression in DTG lungs exposed to Dox (*lane 4*) compared with extremely low levels of CTGF protein expression in STG lungs without (*lane 1*) and with (*lane 3*) Dox treatment and in DTG transgenic lungs without Dox treatment (*lane 2*). (*D*) STG lungs without Dox administration. (*E*) DTG lungs without Dox exposure. (*F*) STG lungs treated with Dox. (*G*) Immunohistochemistry revealed extensive CTGF expression in bronchiolar and alveolar epithelium only in Dox-treated DTG lungs (*arrows*). Magnification, 40×. *Scale bars*, 50 μm.

histological changes similar to those observed in lungs of TGF-β transgenic mice and infants with BPD.

MATERIALS AND METHODS

Generation of Double-Transgenic Mice with Conditional Overexpression of CTGF in Respiratory Epithelium

The study protocols were reviewed and approved by the Animal Care and Use Committee at the University of Miami (Miami, FL). The conditional and tissue specific overexpression of CTGF was achieved by mating two lines of transgenic mice, the CCSP–reverse tetracycline-responsive transactivator (rtTA) mice, bearing the rtTA under the control of the 2.3-kb rat CCSP gene promoter, and the tetracycline operator (TetO)–CTGF mice, containing TetO and minimal cytomegalovirus (CMV) promoter and CTGF transgene (Figure 1A). The CCSP-rtTA mice were provided by Dr. Jeffrey Whitsett (Cincinnati Children's Hospital, Cincinnati, OH), and have been previously described (29, 30). The TetO-CTGF mice were generated in the University of Miami Transgenic Facility. To generate the TetO-CTGF mice, a 1-kb cDNA fragment containing the open reading frame of the human CTGF gene was excised from a pbluescript plasmid construct. The cDNA fragment was blunt-end ligated into the EcoRV site of a plasmid construct containing the Teto-CMV promoter and the bovine growth hormone polyadenylation sequences (provided by Dr. Whitsett). The orientation of the CTGF cDNA insert was confirmed by DNA sequencing. The expression cassette was liberated by nuclease digestion, microinjected into fertilized eggs of C57/B6J mice, and implanted into pseudopregnant host mice, as previously described (30). The transgenic founder mice were identified by PCR reaction of tail DNA with primers, 5′-CCGTACTCCCAAAATCTCCA-3′ and 5′-GCGATGCAATTT CCTCATTT-3′ that span the junction between the TetO and the CTGF cDNA. To generate double-transgenic mice, the homozygous CCSP-rtTA mice were mated to the heterozygous TetO-CTGF mice. The newborn mice were genotyped by PCR of tail DNA with CCSP-rtTA primers, 5′-AAAATCTTGCCAGCTTTCCCC-3′ and 5′-ACTGCCC ATTGCCCAAACAC-3′ and TetO-CTGF primers. To induce CTGF expression in the lungs of newborn pups, the nursing dams were fed with doxycycline containing water (1 mg/ml) from Postnatal Days 1 to 14. Previous studies have demonstrated the efficacy of such feeding regimen in inducing transgene expression (29). Additional litters were given regular drinking water to determine whether CTGF is induced in the absence of doxycycline treatment.

Tissue Preparation

Mice were killed on Postnatal Days 6 and 14, and lungs were infused with 4% paraformaldehyde via a tracheal catheter at 20 cm H_2O of pressure for 5 minutes and then fixed in 4% paraformaldehyde solution overnight at 4°C. Fixed lung tissues were paraffin embedded and 5-μm sections were processed. Additional lungs were also collected for total RNA and protein isolation.

Lung Histology, Morphometry, and Histochemistry

Lung tissue sections were stained by standard hematoxylin and eosin method for histology and morphometry. Morphometric analysis was performed by MetaMorph Imaging System (Molecular Devices, Sunnyvale, CA). Briefly, five random images were taken under 20× magnification on each hematoxylin and eosin–stained lung tissue section. The images were thresholded using equal threshold levels for all groups to obtain consistent results. To determine the mean alveolar airspace area, the air spaces were distinguished from tissues based on intensity, and the number of pixels acquired for each air space was converted to square micrometers (31). To determine the mean cord length (MCL), the images were viewed under a field of equally spaced vertical lines. The MCL was calculated as the average of total length of lines overlying alveolar air space in each image (32). The secondary septa were manually counted on the same images and expressed as the average of total number of secondary septa per image. Lung tissue

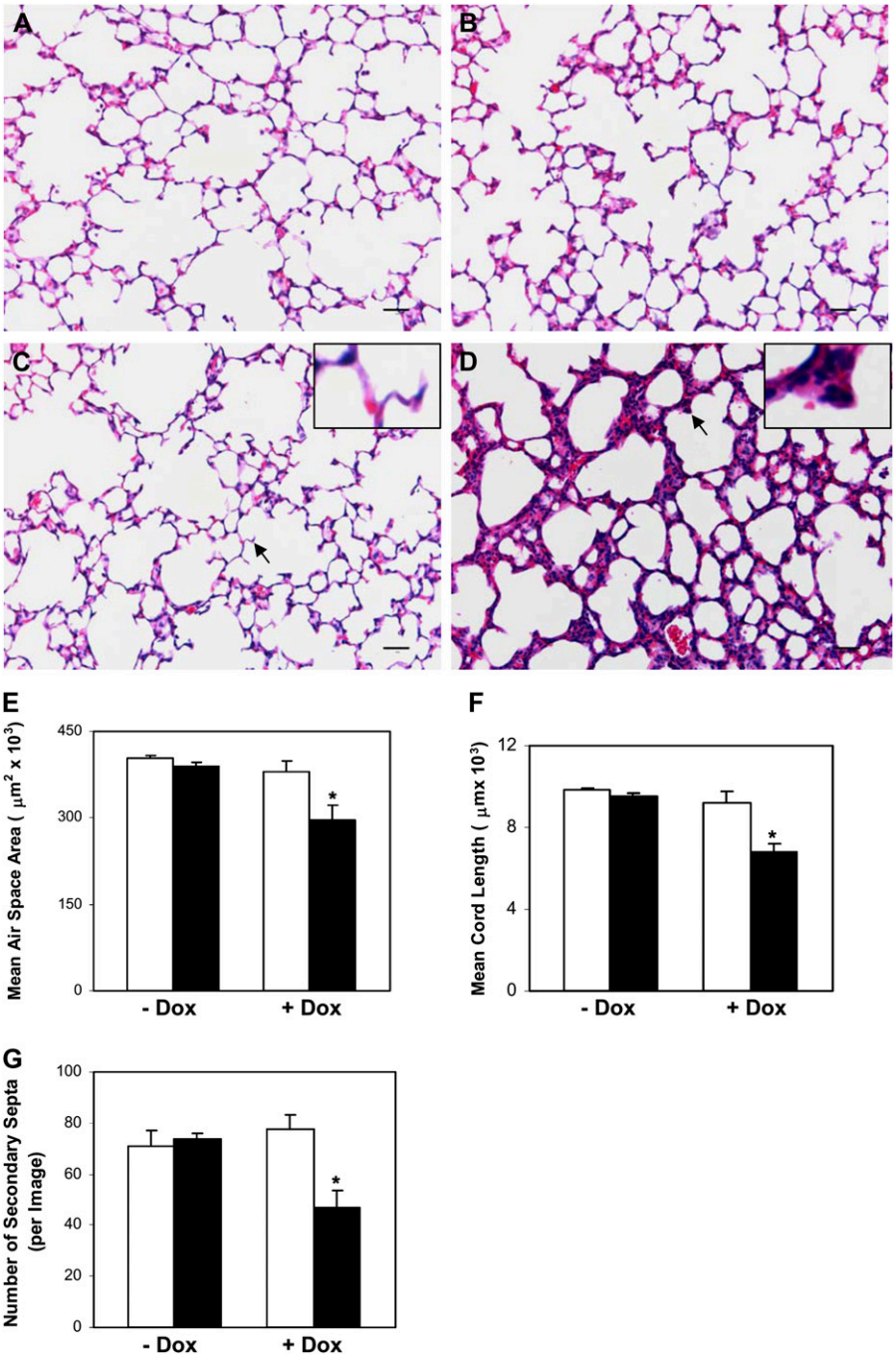

Figure 2. CTGF disrupted alveolarization. Histological examination on hematoxylin and eosin (H&E)–stained lung tissue sections at Postnatal Day 14 demonstrated normal alveolar morphogenesis with thin septa and well formed secondary septa in STG lungs without (*A*) and with (*C*) Dox administration, and in DTG lungs without (*B*) Dox exposure. Administration of Dox disrupted alveolarization with hypercellular septa and poorly formed secondary septa in DTG lungs (*D*). Mean alveolar airspace area (*E*), mean chord length (MCL) (*F*), and number of secondary septa (*G*) were significantly decreased in Dox-treated DTG lungs at Postnatal Day 14. Similar changes in lung histology (STG [*H*]; DTG [*I*]), mean alveolar airspace area (*J*), MCL (*K*), and number of secondary septa (*L*) were detected as early as Postnatal Day 6 after Dox treatment. *Insets* are higher magnification views of secondary septa indicated by the *arrows*. $n = 3$ in groups without Dox administration; $n = 4$ in groups with Dox administration at Postnatal Day 14; $n = 4$ in STG group; and $n = 5$ in DTG group at Postnatal Day 6. *Open bars*, STG; *solid bars*, DTG; * $P < 0.001$, ** $P < 0.005$. Magnification, 20×. *Scale bars*, 50 μm.

sections were also stained with Hart's staining to detect elastic fiber and Picro Sirius Red staining to detect collagen.

Immunohistochemistry and Immunofluorescence Staining

The primary antibodies used in immunohistochemistry and immunofluorescence staining included: goat anti-CTGF and anti–CCSP 10 kD antibodies from Santa Cruz Biotechnology (Santa Cruz, CA); a mouse anti–α–smooth muscle actin (α-SMA) antibody from Sigma (St. Louis, MO); a rabbit anti–pro–SP-C and a goat anti-ILK antibody from Chemicon (Temecula, CA); a rat anti–platelet endothelial cell adhesion molecule (PECAM)–1 antibody from BD Biosciences (San Jose, CA) and an anti–phosphorylated Akt (p-Akt) antibody from Cell Signaling Technology Inc. (Danvers, MA). Briefly, tissue sections were deparaffinized in xylene and rehydrated through graded ethanol into PBS. The sections were incubated with respective primary antibodies overnight at 4°C. For immunohistochemistry, the tissue sections were then incubated with biotinylated secondary IgGs for 1 hour at room temperature. The cell-bound biotinylated secondary antibodies were detected with either streptavidin–biotin–alkaline phosphatase complexes and substrates or streptavidin–biotin–peroxidase complexes and 3,3'-diaminobenzidine (DAB) substrates (Vector, Burlingame, CA). For immunofluorescence staining, the tissue sections were then incubated with AlexaFluor 488– or AlexaFluor 594–labeled secondary antibodies (Invitrogen, Carlsbad, CA) for 1 hour at room temperature. After being washed with PBS, the tissue sections were counterstained with 4′,6-diamidino-2-phenylindole (DAPI; Vector) and mounted with glycerol.

Measurement of Capillary Density

Capillary density was quantified by measuring the area of PECAM-1 immunostaining relative to the total area of alveolar tissue with MetaMorph Imaging System (Molecular Devices), as previously described (33).

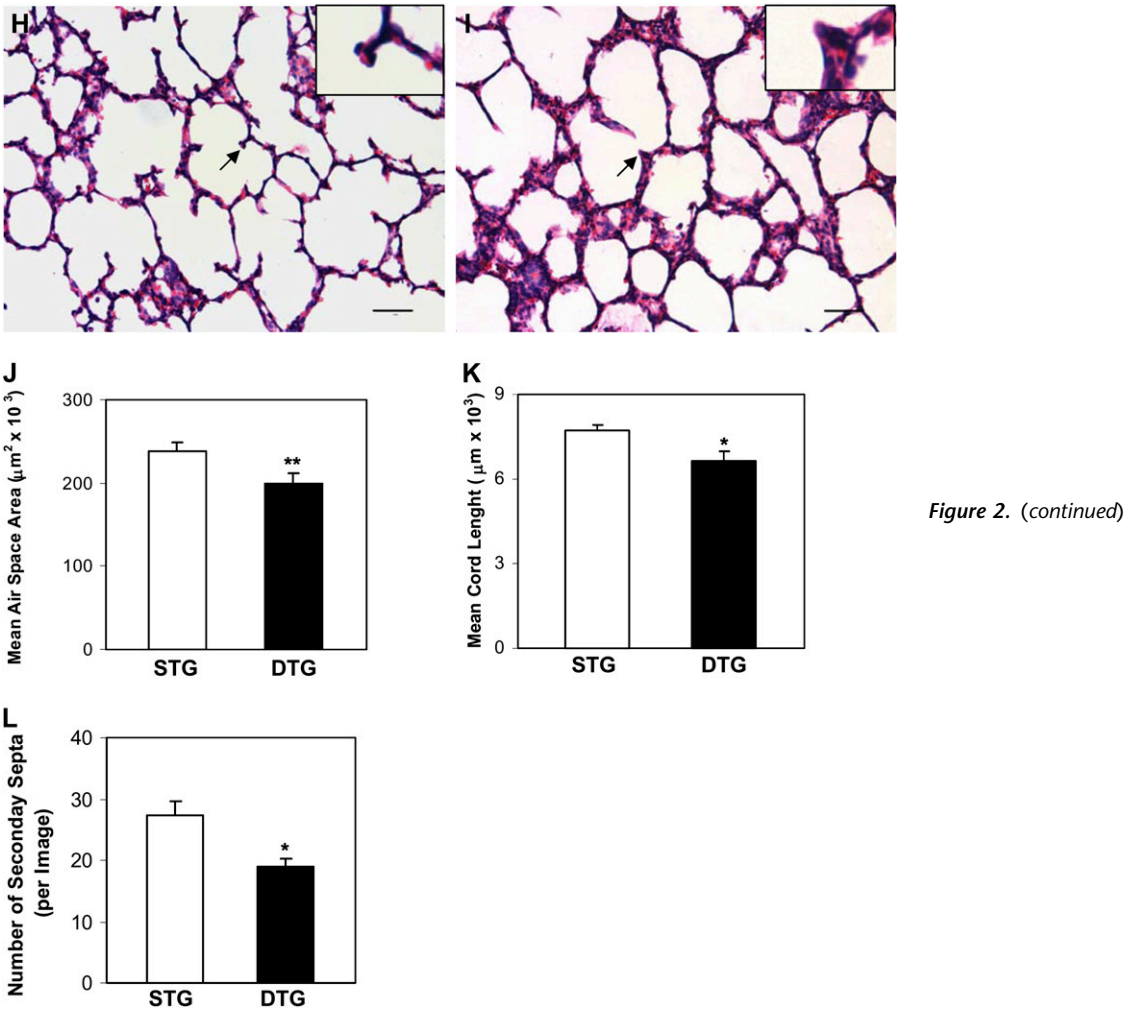

Figure 2. (*continued*)

Cell Proliferation and Apoptosis

Proliferating cells were identified by immunofluorescence staining with an anti–proliferating cell nuclear antigen (PCNA) antibody (Santa Cruz Biotechnology). Apoptotic cells were detected by a terminal deoxynucleotidyl transferase–mediated deoxyuridine triphosphate nick end-labeling (TUNEL) kit according to the manufacturer's protocol (Roche Applied Science, Indianapolis, IN). The tissue sections were counter stained with DAPI to identify all nuclei. The PCNA- and TUNEL-positive nuclei (red signals) and DAPI-stained nuclei (blue) were examined under a fluorescent microscope in 10–12 randomly selected fields from each section. The proliferating or apoptotic cell index was expressed as the ratio of proliferating or apoptotic nuclei to DAPI stained nuclei.

Western Blot Analysis

Total protein was extracted from frozen lung tissues with a RIPA buffer according to manufacturer's protocol (Santa Cruz Biotechnology). The protein concentrations were measured by BCA protein assay using a commercial kit from Pierce Biotechnology Inc. (Rockford, IL). Samples of total protein (50–100 μg) were fractionated by SDS-PAGE on 4–12% Tris-glycine precast gradient gels (Invitrogen) and then transferred to nitrocellulose membranes (Amersham, Piscataway, NJ). The membranes were incubated overnight at 4°C with respective primary antibodies for CTGF, vascular endothelial growth factor (VEGF) (Santa Cruz Biotechnology), ILK, and p-Akt, and then incubated for 1 hour at room temperature with horseradish repoxidase–conjugated secondary antibodies. Antibody-bound proteins were detected with enhanced chemiluminescence methodology (Amersham). Membranes were then stripped with 0.2 N NaOH and reincubated with primary antibodies reactive with a normalization protein, β-actin, and total Akt. The intensities of protein bands were quantified by Quantity One Imaging Analysis Program (Bio-Rad, Hercules, CA).

RNA Isolation and Quantitative Real-Time RT-PCR

Total RNA was isolated from frozen lung tissues and treated with DNase to remove possible DNA contamination, as previously described (25). Total RNA (1 μg) was reverse transcribed in a 20-μl reaction by using a first-strand cDNA synthesis kit according to manufacturer's protocol (Invitrogen). The real-time RT-PCR was performed on an ABI Fast 7500 System (Applied Biosystems, Foster City, CA). Each reaction included diluted first-strand cDNA, CTGF, α-SMA, collagen type I, α1 (col1a1), fibronectin, elastin, emilin 1 or β-actin primers, and master mix containing TaqMan probes, according to the manufacturer's instructions (Applied Biosystems). Real-time RT-PCR conditions were 95°C for 10 minutes, followed by 40 cycles of 95°C for 15 seconds, and 60°C for 30 seconds. RNase-free water was used as a negative control. For each target gene, a standard curve was established by performing a series of dilutions of the first-strand cDNA. The mRNA expression levels of target genes were determined from the standard curve and normalized to β-actin.

Data Presentation and Statistical Analysis

Results are expressed as means (±SD). Comparison between two groups was performed with Student's *t* test. Comparison among four groups was performed by one-way ANOVA, followed by Student-Newman-Keuls test. A *P* value less than 0.05 was considered significant.

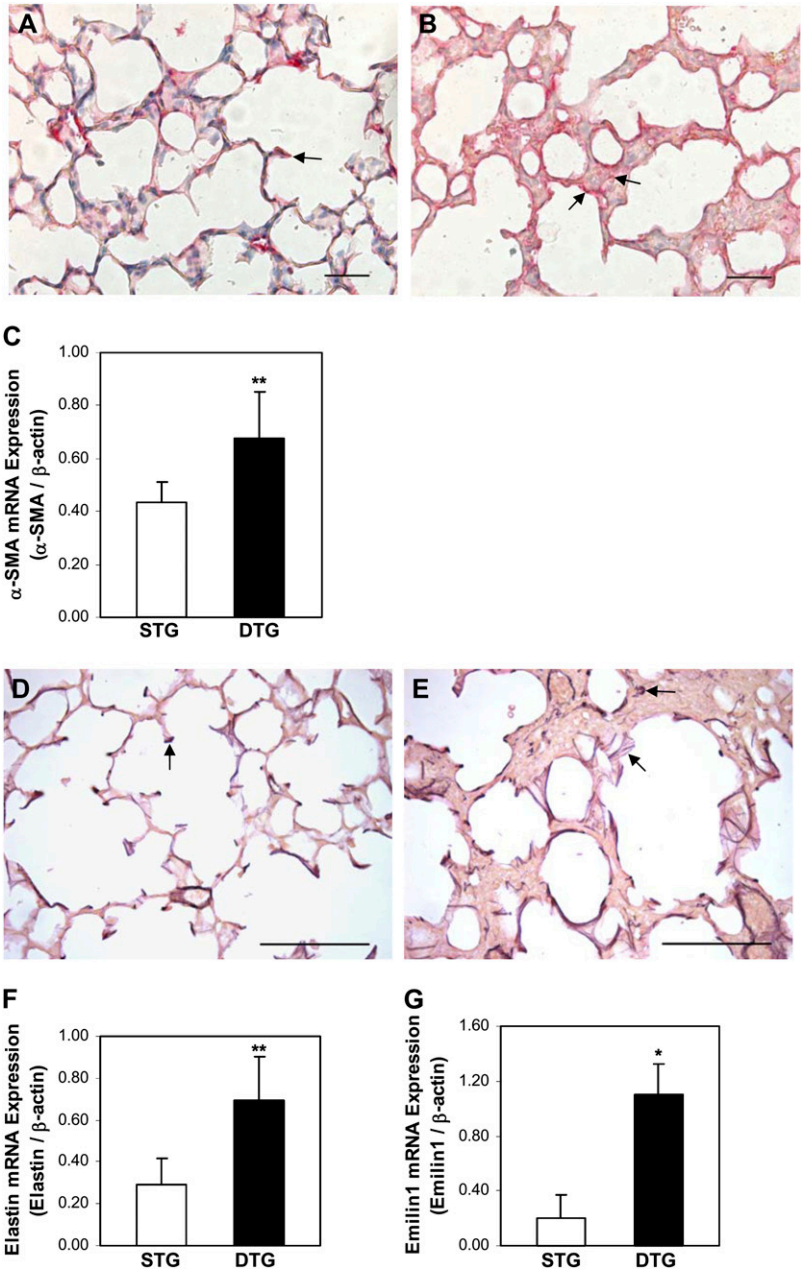

Figure 3. CTGF increased myofibroblast differentiation and caused abnormal elastic fiber deposition in alveolar septa. Immunohistochemistry detected α–smooth muscle actin (α-SMA) expression in cells at the tips of secondary septa in Dox-exposed STG lungs (*arrow* [*A*]). In Dox-exposed DTG lungs, α-SMA was detected irregularly and with increased abundance in alveolar septa and on the surface of alveolar septa (*arrows* [*B*]). (*C*) Quantitative real-time RT-PCR revealed significant increase in α-SMA mRNA expression in Dox-treated DTG lungs. Hart's staining detected organized elastin fibers at the tips of secondary septa and along parts of alveolar septa in Dox-treated STG lungs (*arrow* [*D*]). In Dox-treated DTG lungs, elastin fibers were localized along alveolar septa, at poorly formed secondary septa that are fragmented and irregular, and in thick alveolar septa (*arrows* [*E*]). Quantitative real-time RT-PCR analysis demonstrated increased mRNA expressions of elastin (*F*) and emilin1 (*G*) in Dox-exposed DTG lungs. $n = 4$/group; $^{*}P < 0.001$, $^{**}P < 0.05$. Magnification, 40×. *Scale bars*, 50 μm (*A* and *B*), 100 μm (*D* and *E*).

RESULTS

Conditional Overexpression of CTGF in Respiratory Epithelial Cells of the Postnatal Lung

Mating CCSP-rtTA mice to TetO-CTGF mice produced single-transgenic pups containing CCSP-rtTA or TetO-CTGF, and double-transgenic pups containing both CCSP-rtTA and TetO-CTGF transgenes, which were identified by PCR of tail DNA with CCSP-rtTA and $(TetO)_7$-CTGF primers (Figure 1B). Western blot analysis demonstrated extremely low levels of CTGF protein in lungs from CCSP-rtTA single-transgenic mice with or without doxycycline administration, and from double-transgenic mice without doxycycline administration (Figure 1C). However, treatment with doxycycline for 14 days from Postnatal Day 1 induced high-level expression of CTGF protein in double-transgenic lungs (Figure 1C). Immunohistochemical analysis confirmed that CTGF is undetectable in lungs from single-transgenic mice with or without doxycycline treatment and double-transgenic mice without doxycycline administration (Figures 1D–1F). Intensive expression of CTGF was detected in the nonciliated proximal airway epithelium and in subsets of alveolar epithelial cells in double-transgenic lungs (Figure 1G). Thus, we have generated a mouse model with doxycycline-inducible overexpression of CTGF in respiratory epithelium, and there was no leakage of transgene. Mice survived during the 2 weeks of administration of doxycycline. Body weights were similar between the single- and double-transgenic mice (11.18 ± 1.75 versus 10.24 ± 1.57; $P = 0.24$).

Conditional Overexpression of CTGF Disrupted Alveolarization

Overexpression of CTGF from Postnatal Days 1 to 14 resulted in dramatic changes of lung structure. On histologic examination at Postnatal Day 14, the single-transgenic lungs with or without doxycycline exposure, and the double-transgenic lungs

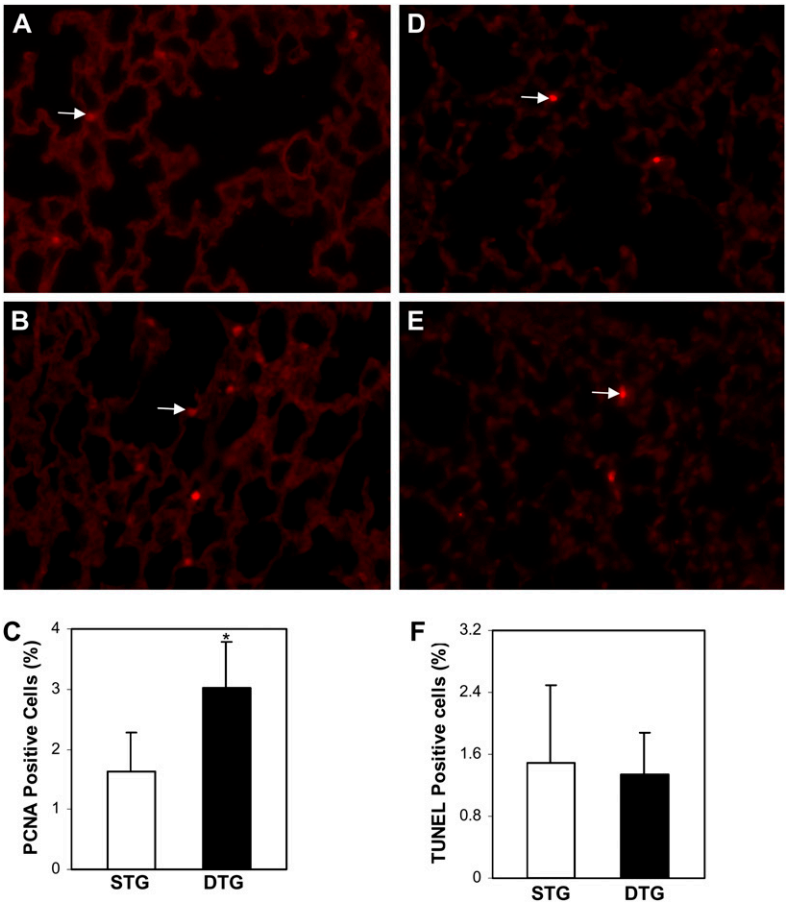

Figure 4. Effects of CTGF on cell proliferation and apoptosis. Immunofluorescence staining with an anti–proliferating cell nuclear antigen (PCNA) antibody detected proliferating cells (*arrows*) in Dox-administrated STG (*A*) and DTG (*C*) lungs. (*D*) Quantification of proliferating cell index demonstrated increased proliferating cells in Dox-treated DTG lungs. Apoptotic cells (*arrows*) were detected by a TUNEL assay in Dox administrated STG (*B*) and DTG (*D*) lungs. (*F*) Quantification of apoptotic index revealed no difference in these lungs. $n = 4$/group; $^*P < 0.05$. Magnification, 40×.

without doxycycline treatment, displayed normal alveolar development (Figures 2A–2C), suggesting that neither doxycycline exposure nor CCSP-rtTA/TetO-CTGF double transgenes alone affects lung development. However, there were simplified alveoli accompanied by hypercellular septa in the double-transgenic lungs exposed to doxycycline (Figure 2D). Further morphometric analysis demonstrated a 27% and a 31% decrease in the mean alveolar airspace area and MCL, respectively, in double-transgenic lungs treated with doxycycline compared with the single-transgenic lungs with or without doxycycline exposure and the double-transgenic lungs without doxycycline treatment (Figures 2E and 2F). The secondary septa were also decreased by 34% (Figure 2G). These histological and morphological changes were also observed at Postnatal Day 6, but to a lesser extent (Figures 2H–2L). Thus, overexpression of CTGF in respiratory epithelium disrupted alveolarization in postnatal lungs. Because the most dramatic changes of lung histology and morphology were detected at Postnatal Day 14 compared with Postnatal Day 6, the following analyses were performed at Postnatal Day 14.

Conditional Overexpression of CTGF Increased Myofibroblast Differentiation, Leading to Disorganized Elastic Fiber Deposition

Alveolar myofibroblasts plays a pivotal role in normal alveolar development. Myofibroblasts located at the tip of secondary crests produce elastin that is crucial for alveolar septation. Alveolar myofibroblasts express α-SMA; we therefore examined α-SMA expression and elastin deposition in lung tissues from doxycycline-treated mice to determine the mechanisms of CTGF-induced abnormal alveolar development. As demonstrated in Figure 3, α-SMA was localized in the cells at the tips of secondary septa in single-transgenic lungs (Figure 3A). In contrast, cells positively stained for α-SMA were detected on alveolar surfaces and in alveolar septa in double-transgenic lungs (Figure 3B). Expression of α-SMA mRNA was increased by 40% in double-transgenic lungs (Figure 3C). These results suggest that overexpression of CTGF increases myofibroblast differentiation in alveolar septa in postnatal lungs. To discern whether increased myofibroblast differentiation alters elastin expression, Hart's staining on lung tissue sections was performed to examine elastin deposition. In single-transgenic lungs, elastin was detected in an organized fashion at the tips of secondary septa and in portions of the alveolar surfaces (Figure 3D). However, in double-transgenic lungs, elastin was detected with increased intensity and disorganized fashion on alveolar surfaces and in septa (Figure 3E). We analyzed mRNA expression of elastin and found a nearly threefold increase in double-transgenic lungs (Figure 3F). We also analyzed mRNA expression of emilin 1, an elastin-related gene, and found more than fivefold increases in double-transgenic lungs. Therefore, increased alveolar myofibroblast differentiation caused by CTGF leads to increased and disorganized elastic fiber deposition in the postnatal lungs, and this may play a role in CTGF disruption of alveolarization.

Effect of Conditional Overexpression of CTGF on Cell Proliferation, Apoptosis, and Epithelial Cell Differentiation

To further determine the mechanisms of CTGF disruption of alveolarization and thickening of septum, cell proliferation was examined by immunofluorescence staining with a PCNA-specific antibody on lung tissue sections from doxycycline-

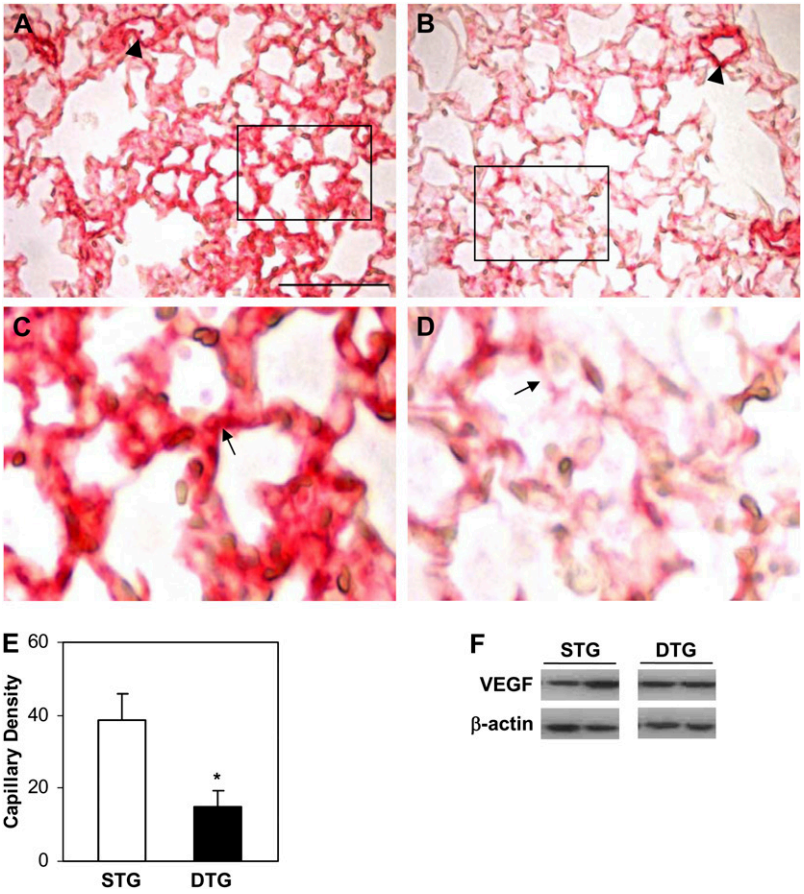

Figure 5. CTGF disrupted capillary development. Immunohistochemistry using an anti–platelet endothelial cell adhesion molecule (PECAM)–1 antibody detected intense signal in intra-acinous vessels (*arrowhead*) and capillary networks (*arrow*) in Dox-treated STG lungs (*A* and *C*). PECAM-1 was detected with intense signal in intra-acinous vessels (*arrowhead*) but with dramatically decreased intensity and continuity in capillary networks (*arrow*) in Dox treated DTG lungs (*B* and *D*). (*E*) Quantification of capillary density determined by the percentage of PECAM-1–stained area versus alveolar tissue area. (*F*) Western blot analysis of vascular endothelial growth factor (VEGF) protein expression. $n = 4$/group; $^*P < 0.01$. Magnification, 40×. *Scale bars*, 100 μm.

treated single- and double-transgenic mice. The proliferating cell index was increased 48% in the alveolar septa in double-transgenic lungs (Figures 4A–4C). TUNEL staining demonstrated few apoptotic cells, and there was no difference between the two groups (Figures 4D–4F). To determine the effect of CTGF on airway epithelial cell and alveolar type II cell differentiation, protein expression of CCSP and pro–SP-C were examined in lung tissue sections from doxycycline-treated single- and double-transgenic mice. The localization and intensity of CCSP and pro–SP-C stainings were similar between the single- and double-transgenic lungs (data not shown).

Overexpression of CTGF Decreased Capillary Formation

To determine the effect of CTGF on pulmonary vascular development, expression of PECAM-1, a surface marker for endothelial cells, was assessed by immunohistochemistry in doxycycline-treated single- and double-transgenic lungs. In single-transgenic lungs, PECAM-1 staining revealed extensive capillary networks located in the thin alveolar septa (Figures 5A and 5C). PECAM-1 was also detected with intense signal in intra-acinous blood vessels (Figure 5A). In double-transgenic lungs, PECAM-1 was detected with strong intensity in intra-acinous blood vessels, which was similar to the control lungs (Figure 5B). However, PECAM-1 staining was dramatically decreased in the capillary networks in alveolar septa (Figures 5B, 5D, and 5E). Quantification of capillary density confirmed the immunohistochemistry finding. Western blot analysis was performed to examine VEGF expression, and showed no significant difference between single- and double-transgenic lungs (Figure 5F).

Overexpression of CTGF Leads to Fibrosis

Histological examination was performed on lung tissue sections from doxycycline-exposed single- and double-transgenic mice. Overexpression of CTGF resulted in dramatic thickening in the peribronchial/peribronchiolar and perivascular regions in double-transgenic lungs (Figure 6B). Special staining for collagen with Picro Sirius Red revealed increased collagen deposition in these regions (Figure 6D). Expression of (col1a1) mRNA was also increased in the double-transgenic lungs (Figure 6E). The expansion of the interstitial myofibroblast population plays a critical role in excessive deposition of ECM. Dual immunofluorescence staining was performed with CTGF- and α-SMA–specific antibodies, and detected increased α-SMA–positive cells in bronchial/bronchioles and blood vessels adjacent to CTGF-expressing cells in double-transgenic lungs (Figure 7). There were also α-SMA–expressing cells detected in the surrounding mesenchyme (Figure 7). These results indicate that overexpression of CTGF induces fibrosis.

Overexpression of CTGF Activates ILK Signaling

To further investigate the potential signaling pathways mediating CTGF-induced abnormal lung development and remodeling, immunohistochemistry and Western blot were performed to examine ILK expression and Akt phosphorylation, a signaling molecule downstream of ILK (19), in lung tissues from doxycycline-administered single- and double-transgenic mice. In single-transgenic lungs, ILK was sparsely detected with weak intensity in bronchiolar epithelial cells (Figure 8A). However, ILK was abundantly detected with strong intensity in bronchiolar epithelial cells and with weak intensity in surrounding

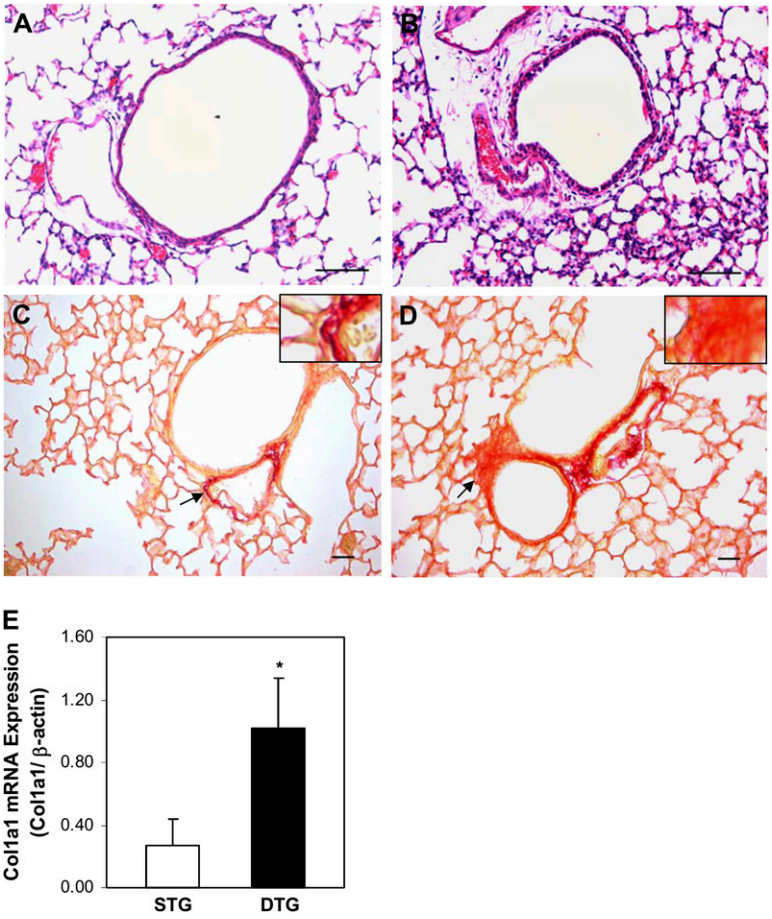

Figure 6. CTGF induced fibrosis. Histologic examination on H&E-stained lung tissue sections revealed dramatic thickening of peribronchial/peribronchiolar and perivascular regions in Dox-administrated DTG lungs (*B*) compared with STG lungs (*A*). Picro Sirius Red staining demonstrated increased collagen deposition in these regions in DTG lungs (*D*) compared with STG lungs (*C*). *Insets* are higher magnification views of the area indicated by the *arrows*. Quantitative real-time RT-PCR demonstrated significantly increased mRNA expression of collagen type I, α1 (col1a1) (*E*) in DTG lungs. $n = 4$/group; $^*P < 0.01$. Magnification, 40× (*A* and *B*), 20× (*C* and *D*). *Scale bars*, 50 μm.

mesenchymal tissues and alveolar septa in double-transgenic lungs (Figure 8B). Western blot analysis confirmed that expression of ILK protein was increased in double-transgenic lungs (Figure 8C). Correlating with ILK expression, p-Akt was undetectable in control lungs (Figure 8D), but strongly detected in bronchiolar epithelial cells and weakly detected in surrounding mesenchymal tissues and alveolar septa in double-transgenic lungs (Figure 8E). Enhanced Akt phosphorylation in double-transgenic lungs was also demonstrated by Western blot analysis (Figure 8F). Fibronectin is one of the target genes of ILK–Akt signaling; we therefore examined fibronectin mRNA expression, and demonstrated a nearly threefold increase in double-transgenic lungs (Figure 8G). These data suggest that ILK–Akt signaling may mediate CTGF responses in postnatal lung development and remodeling.

DISCUSSION

In the present study, we investigated the role of CTGF in postnatal lung development and remodeling with a doxycycline-inducible double-transgenic mouse model to overexpress CTGF in respiratory epithelial cells under the direction of the CCSP gene promoter. We demonstrated for the first time that overexpression of CTGF in the lungs of postnatal mice during the first 2 weeks of life disrupts alveolarization and capillary formation and induces fibrosis. These findings are similar to the histological changes observed in lungs of infants with BPD.

The lung structure of premature infants born at 24 to 28 weeks gestational age, who are at high risk for BPD, is at later canalicular and early saccular stage, with minimal airspace and thick saccular wall (4, 34). Mechanical ventilation and oxygen exposure play a key role in the pathogenesis of BPD, leading to deranged lung development and remodeling. We and others have previously demonstrated that both mechanical ventilation with high tidal volume and oxygen exposure up-regulate CTGF expression in the postnatal rat lungs (25, 26). Moreover, chronic hyperoxia exposure of newborn mice from Postnatal Days 1 to 14 impaired alveolarization that correlates with activation of TGF-β signaling and induction of CTGF gene expression (35). Taken together, these results suggest a potential role of CTGF in the pathogenesis of BPD. The lung of the newborn mouse is at the saccular stage, which will rapidly form alveoli in the first 2 weeks of life (36). Although CTGF gene expression was detected, CTGF protein expression was extremely low during this period. We therefore used the doxycycline-inducible double-transgenic mouse model to overexpress CTGF in respiratory epithelial cells from Postnatal Days 1–14 to study the effects of aberrant CTGF expression on alveolarization and remodeling. The CCSP-rtTA–directed overexpression of CTGF was detected primarily in the nonciliated bronchial and bronchiolar epithelial cells, as well as in subsets of alveolar type II cells, which is similar to the results of previous studies using the same promoter system (29, 30). Our previous study demonstrated that mechanical ventilation with high tidal volume induces CTGF expression in bronchiolar epithelium and alveolar septa (25). Therefore, the expression pattern observed in this study would provide an ideal model to study the effects of CTGF overexpression on postnatal lung development and remodeling. Indeed, our data have provided compelling evidence that links CTGF with abnormal postnatal lung development and remodeling.

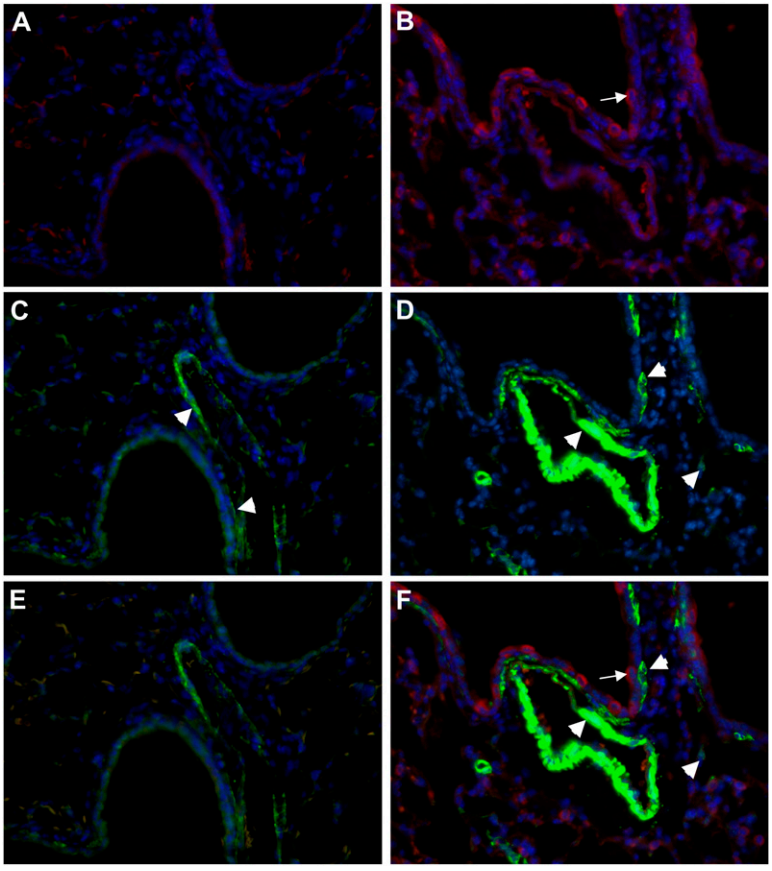

Figure 7. CTGF increased α-SMA expression in mesenchymal tissues surrounding conducting airways and blood vessels. Dual immunofluorescence staining was performed on lung tissue sections from Dox-administrated STG and DTG lungs with an anti-CTGF antibody (*red signal*) and an anti–α-SMA antibody (*green signal*) and DAPI nuclear staining (*blue signal*). CTGF (*A*) was undetectable and α-SMA (*arrowheads* [*C*]) was detected in bronchial/bronchiolar walls and vessels in STG lungs. In DTG lungs, CTGF (*arrow* [*B*]) was detected in airway epithelium and α-SMA (*arrowheads* [*D*]) was detected with increased intensity in bronchial/bronchiolar walls adjacent to CTGF-expressing cells, and in vessels and surrounding mesenchymal tissues. *E* represents a merged image of *A* and *C*; and *F* represents a merged image of *B* and *D*. Magnification, 40×.

We have demonstrated that overexpression of CTGF during the critical alveolar developing period disrupts alveolarization. Fewer and simplified alveoli accompanied by hypercellular septa were observed in doxycycline-administrated double-transgenic lungs at Postnatal Days 6 and 14. Morphometric analysis indicated decreased alveolar airspace area in these lungs. The alveolar development was normal in single-transgenic lungs with or without doxycycline treatment, and in double-transgenic lungs without doxycycline exposure. These data indicate that the lung abnormalities observed in this model are not caused by the off-target effects of CCSP-rtTA or doxycycline toxicity. In the developing lung, alveoli are created by the formation of secondary septa that divide the terminal air spaces into thin-walled sacs. Proper formation of secondary septa requires the participation of alveolar myofibroblasts at the tips of developing alveolar septa. These myofibroblasts actively express elastin, and a well organized temporal elastic fiber formation and deposition are critical for alveolar septation and normal alveolar development (37–39). In mice deficient for platelet-derived growth factor, there is a lack of myofibroblasts at the tips of the alveolar septa, and, consequently, a lack of elastin fiber deposition, leading to dilated and thin-walled distal air sacs in neonatal lungs (40). In contrast, in a triple-transgenic mouse model, overexpression of TGF-β in airway epithelium results in increased myofibroblast formation in alveolar septa, leading to thick-walled and fewer alveoli at 2 weeks postnatal age (8). Overexpression of CTGF in this model resulted in increased alveolar myofibroblast differentiation resembling that observed in TGF-β transgenic lungs. In addition, overexpression of CTGF increased elastin and emilin 1 mRNA expression, and caused increased and disorganized elastic fiber deposition, as well as poor and decreased secondary septal formation. These data further support the important role of coordinated temporal and spatial myofibroblast differentiation and elastic fiber organization in alveologenesis.

Overexpression of CTGF increased cell proliferation in alveolar septa, but did not affect cell apoptosis or epithelial cell differentiation in the postnatal lungs. Previous studies have demonstrated that CTGF gene mutation results in decreased proliferation and increased apoptosis in lungs of embryos at Embryonic Day 18.5 (28). However, CTGF gene mutation did not change SP-C protein expression, but increased cytoplasmic glycogen, suggesting delayed epithelial cell maturation (28). These results indicate that CTGF plays a more prominent role in regulating cell proliferation than epithelial cell differentiation during embryonic and postnatal lung development.

The impaired alveolarization was associated with abnormal alveolar vascular network formation in this study. Overexpression of CTGF resulted in decreased PECAM-1 expression in the alveolar vascular networks, but did not change PECAM-1 expression in the intra-acinous blood vessels in the postnatal lung. VEGF plays a key role in regulating alveolar epithelial and endothelial interaction, thus leading to the establishment of gas–blood exchange units (41). A recent study demonstrated that selective inactivation of VEGF in respiratory epithelium results in defects in both alveolar septation and capillary formation (42). Previous studies have indicated that CTGF is able to bind to VEGF in the ECM, thus decreasing the VEGF angiogenic effect (43–45). In this study, we have examined VEGF expression, and did not show any differences between the two groups. We speculate that two possible mechanisms are involved in decreased capillary development in this model. First, CTGF produced by the alveolar epithelial cells may bind to VEGF locally, which decreases VEGF binding to its receptors on the capillary endothelial cells, thus decreasing capillary formation. Second, previous studies have demonstrated that impaired alveolarization

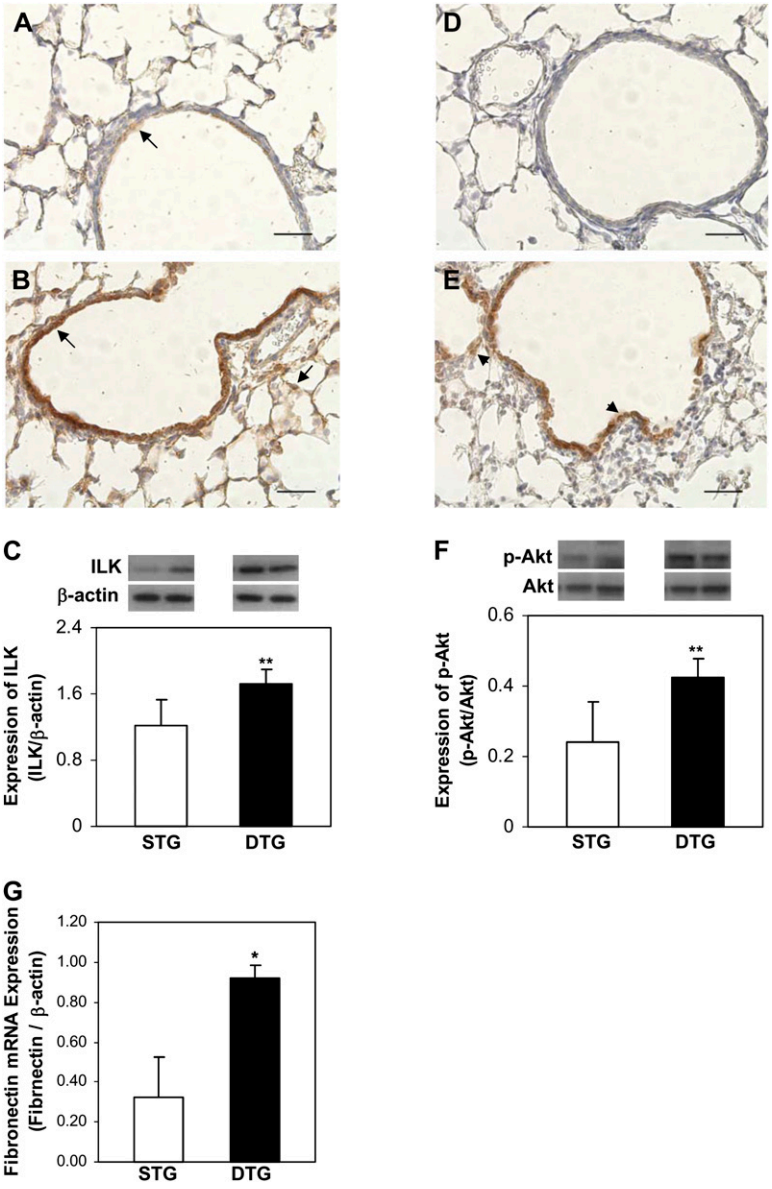

Figure 8. CTGF activated integrin-linked kinase (ILK)–Akt signaling. Immunohistochemistry was performed with anti-ILK and anti–p-Akt antibodies on lung tissue sections from Dox-treated STG and DTG mice. In STG lungs, ILK was detected with low intensity in bronchiolar epithelial cells (*arrow* [*A*]), and p-Akt was undetectable (*D*). In DTG lungs, ILK (*arrows* [*B*]) and p-Akt (*arrowheads* [*E*]) were detected with strong intensity in bronchiolar epithelial cells, and weakly in surrounding mesenchymal tissues and alveolar septa. Western blot demonstrated that overexpression of CTGF increased ILK expression (*C*) and activated Akt (*F*) in DTG lungs. Quantitative real-time RT-PCR demonstrated increased fibronectin mRNA expression in DTG lungs (*G*). $n = 4$/group; $^{*}P < 0.001$, $^{**}P < 0.05$. Magnification, 40×. *Scale bars*, 50 μm.

leads to impaired capillary formation, or *vice versa*. Impaired alveolarization caused by overexpression of CTGF in this model could lead to decreased capillary formation.

Variable interstitial fibrosis is observed in BPD lungs in clinical studies and experimental animal models (4, 46–48). Previous studies have demonstrated the critical role of CTGF in inducing lung fibrosis in adult rats and mice (21, 49). In this study, overexpression of CTGF resulted in lung fibrosis during the critical alveolar developing period. Besides thickening of alveolar septa, there was dramatic thickening in the peribronchial/peribronchiolar and perivascular regions in double-transgenic lungs. The collagen deposition and expression of α-SMA in these regions were dramatically increased by CTGF. CTGF stimulates fibroblast-to-myofibroblast differentiation, as well as epithelial-to-mesenchymal transdifferentiation, leading to fibrosis (50, 51). Future studies are needed to explore the cellular and molecular mechanisms of CTGF-induced alteration of myofibroblast differentiation leading to abnormal alveolar development and fibrosis in postnatal lungs.

We have demonstrated that overexpression of CTGF increases ILK expression in bronchiolar epithelial cells during the alveolar developmental period. ILK is an intracellular serine/threonine protein kinase that couples integrins to downstream signaling pathways involved in a variety of cellular functions during development and remodeling. Increasing evidence indicates that ILK plays a key role in mediating TGF-β– and CTGF-induced renal tubular epithelial-to-mesenchymal transdifferentiation, which is believed to play a critical role in renal interstitial fibrogenesis (52, 53). In cultured human lung fibroblasts, overexpression of ILK induces Akt phosphorylation and protects collagen matrix contraction–induced apoptosis (54). In this study, overexpression of CTGF also enhanced Akt phosphorylation at the sites where ILK was induced. We have also demonstrated that expression of fibronectin mRNA, one of the ILK–Akt downstream target genes, is up-regulated in the double-transgenic lungs. These data suggest that ILK–Akt signaling pathway may be involved in CTGF-induced abnormal postnatal lung development and remodeling.

Taken together, overexpression of CTGF disrupts alveolarization and capillary formation, and induces fibrosis in the postnatal lungs. The simplification of alveolarization and capillary formation induced by CTGF has striking similarity to lung pathologies observed in infants with BPD. The observation of overexpression of CTGF correlating with activation of ILK–

Akt signaling pathway highlights the potential role of the CTGF–ILK–Akt pathway in the pathogenesis of BPD.

Conflict of Interest Statement: E.B. received an institutional research support grant from Viasys ($10,001–$50,000) and has a patent for an automated oxygen controller. As a result of a licensing agreement he received royalties from Viasys ($5,001–$10,000). None of the other authors has a financial relationship with a commercial entity that has an interest in the subject of this manuscript.

Acknowledgments: The authors thank Dr. Matthew Duncan for his excellent support in performing platelet endothelial cell adhesion molecule–1 immunohistochemistry.

References

1. Jobe AH, Bancalari E. Bronchopulmonary dysplasia. *Am J Respir Crit Care Med* 2001;163:1723–1729.
2. Husain AN, Siddiqui NH, Stocker JT. Pathology of arrested acinar development in post surfactant bronchopulmonary dysplasia. *Hum Pathol* 1998;29:710–717.
3. Coalson JJ, Winter VT, Delemos RA. Decreased alveolarization in baboon survivors with bronchopulmonary dysplasia. *Am J Respir Crit Care Med* 1995;152:640–646.
4. Coalson JJ. Pathology of bronchopulmonary dysplasia. *Semin Perinatol* 2006;30:179–184.
5. Jobe AJ. The new BPD: an arrest of lung development. *Pediatr Res* 1999;46:641–643.
6. Kotecha S, Wangoo A, Silverman M, Shaw R. Increase in the concentration of transforming growth factor beta-1 in bronchoalveolar lavage fluid before development of chronic lung disease of prematurity. *J Pediatr* 1996;128:464–469.
7. Lecart C, Cayabyab R, Buckley S, Morrison J, Kwong K, Warburton D, Ramanathan R, Jones C, Minoo P. Bioactive transforming growth factor–beta in the lungs of extremely low birth weight neonates predicts the need for home oxygen supplementation. *Biol Neonate* 2000;77:217–223.
8. Vicencio AG, Lee CG, Cho SJ, Eickelberg O, Chuu Y, Haddad GG, Elias JA. Conditional overexpression of bioactive transforming growth factor-beta1 in neonatal mouse lung: a new model for bronchopulmonary dysplasia? *Am J Respir Cell Mol Biol* 2004;31: 650–656.
9. Grotendorst GR. Connective tissue growth factor: a mediator of TGF-beta action on fibroblasts. *Cytokine Growth Factor Rev* 1997;8:171–179.
10. O'Brien TP, Yang GP, Sanders L, Lay LF. Expression of cyr61, a growth factor–inducible immediate early gene. *Mol Cell Biol* 1990;10:3569–3577.
11. Bork P. The modular architecture of a new family of growth regulators related to connective tissue growth factor. *FEBS Lett* 1993;327:125–130.
12. Leask A, Abraham DJ. All in the CCN family: essential matricellular signaling modulators emerge from the bunker. *J Cell Sci* 2006;119: 4803–4810.
13. Nishida T, Kamaki H, Baxter RM, DeYoung RA, Takigawa M, Lyons KM. CCN2 (connective tissue growth factor) is essential for extracellular matrix production and integrin signaling in chondrocytes. *J Cell Commun Signal* 2007;1:45–58.
14. Gao R, Brigstock DR. Connective tissue growth factor (CCN2) induces adhesion of rat activated hepatic stellate cells by binding of its C-terminal domine to integrin αvβ3 and heparin sulfate proteoglycan. *J Biol Chem* 2004;279:8848–8855.
15. Schwartz MA, Ginsberg MH. Networks and crosstalk: integrin signaling spreads. *Nat Cell Biol* 2002;4:E65–E68.
16. Hannigan GE, Fitz-Gibbon CL, Coppolino MG, Radeva G, Filmus J, Bell JC, Dedhar S. Regulation of cell adhesion and anchorage-dependent growth by a new β1-integrin–linked protein kinase. *Nature* 1996;379:91–96.
17. Attwell S, Mills J, Troussard A, Wu C, Dedhar S. Integration of cell attachment, cytoskeletal localization, and signaling by integrin-linked kinase (ILK), CH-ILKBP, and the tumor suppressor PTEN. *Mol Biol Cell* 2003;14:4813–4825.
18. Terpstra L, Prud'homme J, Arabian A, Takeda S, Karsenty G, Dedhar S, St-Arnaud R. Reduced chondrocyte proliferation and chondrodysplasia in mice lacking the integrin-linked kinase in chondrocytes. *J Cell Biol* 2003;162:139–148.
19. Qian Y, Zhong X, Flynn DC, Zheng JZ, Qiao Z, Wu C, Dedhar S, Shi X, Jiang X. ILK mediates actin filament rearrangements and cell migration and invasion through PI3K/Akt/Rac1 signaling. *Oncogene* 2005;24:3154–3165.
20. Sato S, Nagaoka T, Hasegawa M, Tamatani T, Nakanishi T, Takigawa M, Takehara K. Serum level of connective tissue growth factor are elevated in patients with systemic sclerosis: association with extent of skin sclerosis and severity of pulmonary fibrosis. *J Rheumatol* 2000;27: 149–154.
21. Bonniaud P, Margetts PJ, Kolb M, Haberberger T, Kelly M, Robertson J, Gauldie J. Adenoviral gene transfer of connective tissue growth factor in the lung induces transient fibrosis. *Am J Respir Crit Care Med* 2003;168:770–778.
22. Xu YD, Hua J, Mui A, O'Connor R, Grotendorst G, Khalil N. Release of biologically active TGF-beta1 by alveolar epithelial cells results in pulmonary fibrosis. *Am J Physiol Lung Cell Mol Physiol* 2003;285: L527–L539.
23. Alejandre-Alcazar MA, Michiels-Corsten M, Vicencio AG, Reiss I, Ryu J, de Krijger RR, Haddad GG, Tibboel D, Seeger W, Eickelberg O, *et al.* TGF-β signaling is dynamically regulated during the alveolarization of rodent and human lungs. *Dev Dyn* 2008;237:259–269.
24. Wu S, Peng J, Duncan MR, Kasisomayajula K, Grotendorst G, Bancalari E. ALK-5 mediates endogenous and TGF-β1–induced expression of connective tissue growth factor in embryonic lung. *Am J Respir Cell Mol Biol* 2007;36:552–561.
25. Wu S, Capasso L, Lessa A, Peng JH, Kasisomayajula K, Rodriguez M, Suguihara C, Bancalari E. High tidal volume ventilation up-regulates CTGF expression in the lung of newborn rats. *Pediatr Res* 2008;63: 245–250.
26. Chen CM, Wang LF, Chou HC, Lang YD, Lai YP. Up-regulation of connective tissue growth factor in hyperoxia-induced lung fibrosis. *Pediatr Res* 2007;62:128–133.
27. Ivkovic S, Yoon BS, Popoff SN, Safadi FF, Libuda DE, Stephenson RC, Daluiski A, Lyons KM. Connective tissue growth factor coordinates chondrogenesis and angiogenesis during skeletal development. *Development* 2003;130:2779–2791.
28. Baguma-Nibasheka M, Kablar B. Pulmonary hypoplasia in the connective tissue growth factor (CTGF) null mouse. *Dev Dyn* 2008;237:485–493.
29. Perl AT, Tichelaar JW, Whitsett JA. Conditional gene expression in the respiratory epithelium of the mouse. *Transgenic Res* 2002;11:21–29.
30. Tichelaar JW, Liu W, Whitsett JA. Conditional expression of fibroblast growth factor–7 in the developing and mature lung. *J Biol Chem* 2000; 275:11858–11864.
31. Liu C, Ikegami M, Stahlman MT, Dey CR, Whitsett JA. Inhibition of alveolarization and alter pulmonary mechanics in mice expression GATA-6. *Am J Physiol Lung Cell Mol Physiol* 2003;285:L1246–L1254.
32. Bry K, Whitsett JA, Lappalainen U. IL-1β disrupts postnatal lung morphogenesis in the mouse. *Am J Respir Cell Mol Biol* 2007;36: 32–34.
33. Maniscalco WM, Watkins RH, Pryhuber GS, Bhatt A, Shea C, Huyck H. Angiogenic factors and alveolar vasculature: development and alterations by injury in very premature baboons. *Am J Physiol Lung Cell Mol Physiol* 2002;282:L811–L823.
34. Massaro GD, Massaro D. Formation of pulmonary alveoli and gas-exchange surface area: quantitation and regulation. *Annu Rev Physiol* 1996;58:73–92.
35. Alejandre-Alcázar MA, Kwapiszewska A, Reiss I, Amarie OV, Marsh LM, Sevilla-Pérez J, Wygrecka M, Eul B, Köbrich S, Hesse M, *et al.* Hyperoxia modulates TGF-β/BMP signaling in a mouse model of bronchopulmonary dysplasia. *Am J Physiol Lung Cell Mol Physiol* 2007;292:L537–L549.
36. Warburton D, Schwarz M, Tefft D, Flores-Delgado G, Anderson KD, Cardoso WV. The molecular basis of lung morphogenesis. *Mech Dev* 2000;92:55–81.
37. Shifren A, Mecham RP. The stumbling block in lung repair of emphysema: elastic fiber assembly. *Proc Am Thorac Soc* 2006;3:428–433.
38. Shifren A, Durmowicz AG, Knutsen RH, Hirano E, Mecham RP. Elastin protein levels are a vital modifier affecting normal lung development and susceptibility to emphysema. *Am J Physiol Lung Cell Mol Physiol* 2007;292:L778–L787.
39. Bland RD, Ertsey R, Mokres LM, Xu L, Jacobson DE, Jiang S, Alvira CM, Rabinovitch M, Shinwell ES, Dixit A. Mechanical ventilation uncouples synthesis and assembly of elastin and increases apoptosis in lungs of newborn mice: prelude to defective alveolar septation during lung development? *Am J Physiol Lung Cell Mol Physiol* 2008;294:L3–L14.

40. Lindahl P, Karlsson L, Hellstrom M, Gebre-Medhin S, Willetts K, Heath JK, Betsholtz C. Alveogenesis failure in PDGF-A–deficient mice is coupled to lack of distal spreading of alveolar smooth muscle cell progenitors during lung development. *Development* 1997;124:3943–3953.
41. Thebaud B, Abman SH. Bronchopulmonary dysplasia: where have all the vessels gone? Roles of angiogenic growth factors in chronic lung disease. *Am J Respir Crit Care Med* 2007;175:978–985.
42. Yamamoto H, Yun EJ, Gerber H, Ferrara N, Whitsett JA, Vu TH. Epithelial–vascular cross talk mediated by VEGF-A and HGF signaling directs primary septae formation during distal lung morphogenesis. *Dev Biol* 2007;308:44–53.
43. Inoki I, Shiomi T, Hashimoto G, Enomoto H, Nakamura H, Makino KI, Ikeda E, Takata S, Kobayashi KI, Okada Y. Connective tissue growth factor binds vascular endothelial growth factor (VEGF) and inhibits VEGF-induced angiogenesis. *FASEB J* 2002;16:219–221.
44. Hashimoto G, Inoko I, Fujii Y, Aoki T, Ikeda E, Okada Y. Matrix metalloproteinases cleave connective tissue growth factor and reactivate angiogenic activity of vascular endothelial growth factor 165. *J Biol Chem* 2002;277:36288–36295.
45. Dean RA, Butler GS, Hamma-Kourbali Y, Delbe J, Brigstock DR, Courty J, Overall CM. Identification of candidate angiogenic inhibitors processed by matrix metalloproteinase 2 (MMP2) in cell-based proteomic screens: disruption of vascular endothelial growth factor (VEGF)/heparin affin regulatory peptide (pleiotrophin and VEGF/connective tissue growth factor angiogenic inhibitory complexes by MMP2 proteolysis. *Mol Cell Biol* 2007;27:8454–8465.
46. Dik WA, De Krijger RR, Bonekamp L, Naber BA, Zimmermann LJ, Versnel MA. Localization and potential role of matrix metalloproteinase–1 and tissue inhibitors of metalloproteinase-1 and -2 in different phases of bronchopulmonary dysplasia. *Pediatr Res* 2001; 50:761–766.
47. Ashour K, Shan L, Lee JH, Schlicher W, Wada K, Wada E, Sunday ME. Bombesin inhibits alveolarization and promotes pulmonary fibrosis in newborn mice. *Am J Respir Crit Care Med* 2006;173: 1377–1385.
48. Viscardi RM, Atamas SP, Luzina IG, Hasday JD, He JR, Sime PJ, Coalson JJ, Yoder BA. Antenatal *Ureaplasma urealyticum* respiratory tract infection stimulates proinflammatory, profibrotic responses in the preterm baboon lung. *Pediatr Res* 2006;60:141–146.
49. Bonniaud P, Martin G, Margetts PJ, Ask K, Robertson J, Gauldie J, Kolb M. Connective tissue growth factor is crucial to inducing a profibrotic environment in "fibrosis-resistant" BALB/c mouse lungs. *Am J Respir Cell Mol Biol* 2004;31:510–516.
50. Grotendorst GR, Rahmanie H, Duncan MR. Combinatorial signaling pathways determine fibroblast proliferation and myofibroblast differentiation. *FASEB J* 2004;18:469–479.
51. Burns WC, Twigg SM, Forbes JM, Pete J, Tikellis C, Thallas-Bonke V, Thomas MC, Cooper ME, Kantharidis P. Connective tissue growth factor plays an important role in advanced glycation end product-induced tubular epithelial-to-mesenchymal transition: implications for diabetic renal disease. *J Am Soc Nephrol* 2006;17:2484–2494.
52. Liu BC, Li MX, Zhang JD, Liu XC, Zhang XL, Phillips AO. Inhibition of integrin-linked kinase via a siRNA expression plasmid attenuates connective tissue growth factor–induced human proximal tubular epithelial cells to mesenchymal transition. *Am J Nephrol* 2008;28: 143–151.
53. Li Y, Yang J, Dai C, Wu C, Liu Y. Role of integrin-linked kinase in mediating tubular epithelial to mesenchymal transition and renal interstitial fibrogenesis. *J Clin Invest* 2003;112:503–516.
54. Nho RS, Xia H, Kahm J, Kleidon J, Diebold D, Henke CA. Role of integrin-linked kinase in regulating phosphorylation of Akt and fibroblast survival in type I collagen matrices through a beta1 integrin viability signaling pathway. *J Biol Chem* 2005;280:26630–26639.